CrossMark

MATISSE first pictures of dust and molecules around R Sculptoris

J. Drevon[1] , **F. Millour**[1], **P. Cruzalèbes**[1], **C. Paladini**[2], **J. Hron**[3],
A. Meilland[1], **F. Allouche**[1], **B. Aringer**[3], **P. Berio**[1], **W.C. Danchi**[4],
V. Hocdé[5], **K.-H. Hofmann**[6], **S. Lagarde**[1], **B. Lopez**[1], **A. Matter**[1],
R. Petrov[1], **S. Robbe-Dubois**[1], **D. Schertl**[6], **P. Stee**[1], **F. Vakili**[1]
J. Varga[7,8], **R. Waters**[9,10], **G. Weigelt**[6], **J. Woillez**[11],
M. Wittkowski[11] and **G. Zins**[2],

[1]Université Côte d'Azur, Observatoire de la Côte d'Azur, CNRS, Laboratoire Lagrange, France
email: julien.drevon@oca.eu

[2]European Southern Observatory, Alonso de Córdova, 3107 Vitacura, Santiago, Chile

[3]Department of Astrophysics, University of Vienna, Türkenschanzstrasse 17

[4]NASA Goddard Space Flight Center, Astrophysics Division, Greenbelt, MD 20771, USA

[5]Nicolaus Copernicus Astronomical Center, Polish Academy of Sciences, Bartycka 18, 00-716
Warszawa, Poland

[6]Max-Planck-Institut für Radioastronomie, Auf dem Hügel 69, D-53121 Bonn, Germany

[7]Konkoly Observatory, Research Centre for Astronomy and Earth Sciences, Eötvös Loránd
Research Network (ELKH), Konkoly-Thege Miklós út 15-17, H-1121 Budapest, Hungary

[8]Leiden Observatory, Leiden University, Niels Bohrweg 2, NL-2333 CA Leiden, The
Netherlands

[9]Department of Astrophysics/IMAPP, Radboud University, P.O. Box 9010, 6500 GL
Nijmegen, The Netherlands

[10]SRON Netherlands Institute for Space Research Sorbonnelaan 2, 3584 CA Utrecht, The
Netherlands

[11]European Southern Observatory, Karl-Schwarzschild-Str. 2, 85748 Garching, Germany

Abstract. Carbon-rich dust is known to form in the atmosphere of the semiregular variable star R Sculptoris. Such stardust, as well as the molecules and gas produced during the lifetime of the star, will be spread into the Galaxy via the mass-loss process. Probing this process is crucial to understand the chemical enrichment of the Galaxy. R Scl was observed using the ESO/VLTI MATISSE instrument in December 2018. Here we show the first images of the star between 3 and $10\,R_\star$. Using the complementary `MIRA` 3D image reconstruction and the `RHAPSODY` 1D intensity profile reconstruction code, we reveal the location of molecules and dust in the close environment of the star. Indeed, the C_2H_2 and HCN molecules are spatially located between 1 and $3.4\,R_\star$ which is much closer to the star than the location of the dust. The R Scl spectrum is fitted by molecules and a dust mixture of 90% of amorphous carbon and 10% of silicone carbide. The inner boundary of the dust envelope is estimated by `DUSTY` at about $4.6\,R_\star$. We derive a mass-loss rate of $1.2 \pm 0.4 \times 10^{-6} M_\odot\ \mathrm{yr}^{-1}$ however no clear SiC forming region has been detected in the MATISSE data.

Keywords. instrumentation: interferometers, stars: AGB and post-AGB, stars: carbon, stars: atmospheres, stars: mass loss, stars: individual: R Scl
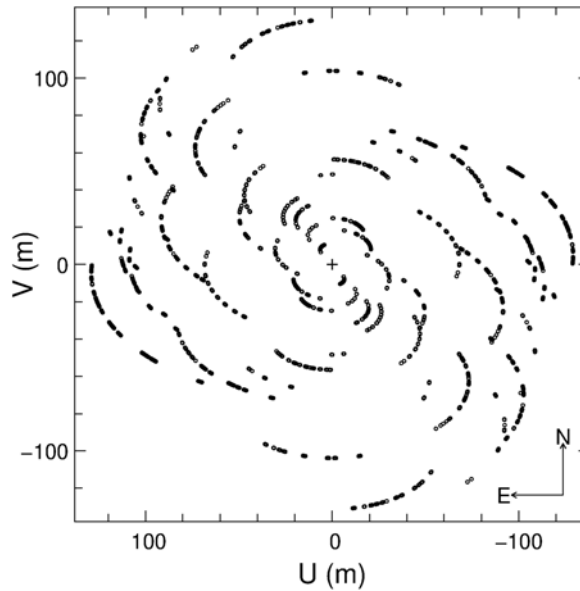
Figure 1. Final (u,v)-plane coverage on R Scl with VLTI/MATISSE. The U and V coordinates are those of the projected baseline vectors.

1. Introduction

R Scl is an Asymptotic Giant Branch (AGB) carbon-rich star known to be a bright infrared and semi-regular pulsation source with a mass-loss rate ranging from $2 \times 10^{-10}\,M_\odot$ yr^{-1} (Brunner et al. 2018), up to $1.6 \times 10^{-6}\,M_\odot$ yr^{-1} (De Beck et al. 2010). The conservative distance of this spectral C-N5-type star used in this proceeding is 360 ± 50 pc estimated by Maercker et al. (2018). R Scl has a pulsation period of about 370 days (Samus et al. 2009) with a C/O≈ 1.4 (Hron et al. 1998). ALMA observations (Maercker et al. 2012) revealed spirals-like, clumpy, and non-centrosymmetric structures inside the shell (also confirmed through polarimetric observations by Yudin & Evans (2002)). These structures can be explained by the presence of an unseen companion of $0.25\,M_\odot$ hidden at 60 au in the dusty shell. Wittkowski et al. (2017) presented PIONIER observation of the surface of the star, reveling an extended photosphere with a dominant spot very likely of convective origin. In addition, Sacuto et al. (2011) observed the stellar environment above 3 $R_\star$ with the MIDI instrument but the uv-plane was not dense enough to use the observations for image reconstruction. Here we fill the gap and use MATISSE to obtain the first simultaneous $L-$ (3–4 μm) and $N-$ (8–13 μm) band observations with a complete uv-plane coverage to make image reconstruction.

2. Data analysis

The observations of R Scl were obtained using the MATISSE instrument (Lopez et al. 2022) mounted at the Very Large Telescope Interferometer (VLTI), in combination with the 4 Auxiliary Telescopes (ATs) in various configurations. The star was observed in December 2018 for about 7 nights (51 hours) optimizing the uv-coverage (see Fig. 1). The data reduction is done using the MATISSE software `drsmat` version 1.5.0 (Millour et al. 2016). MATISSE data were acquired in LOW spectral resolution $L-$ and $N-$ band (R$\sim$30).

Table 1. Parameters of the central source and the dust envelope derived respectively by
`COMARCS` (top part) and `DUSTY` (bottom part).

Model parameter	Parameter value	Fixed
Distance	360 ± 50 pc	Yes
Surface gravity	-0.50 ± 0.10 cm.s^{-2}	No
Stellar surface temperature	2700 ± 100 K	No
Stellar Luminosity	$8000 \pm 1000\,L_\odot$	No
Stellar mass	$2.0 \pm 0.5\,M_\odot$	No
C/O ratio	$2^{+2.0}_{-0.6}$	No
Microturbulent velocity	2.5 km.s^{-1}	Yes
Rosseland Radius	$1.91 \pm 0.20\,au$	No
	5.3 ± 0.6 mas	
Shell chemical composition	AmC and SiC	No
	$88 \pm 11\%$ of AmC	
	$12 \pm 11\%$ of SiC	
Dust grain-size distribution	$n(a) \propto a^{-3.5}$	Yes
Optical depth at $\lambda = 1\ \mu$m	0.19 ± 0.05	No
Inner boundary temperature	1200 ± 100 K	Yes
Inner radius	24.5 ± 9.0 mas	No
	$4.6 \pm 1.7\,R_\star$	
Outer radius	$1000\,R_{in}$	Yes
Mass-loss rate	$1.2 \pm 0.4 \times 10^{-6} M_\odot$ yr^{-1}	No

3. SED fitting

We assume that the star at a given pulsation phase can be described as an hydrostatic `COMARCS` model (Aringer et al. 2016) and a `DUSTY` envelope (Ivezić & Elitzur 1996). To obtain the stellar parameters, we first fit the dereddened photometry (between *V*- and *I*-band) with 2600 synthetic observations. The latter are derived from 1D hydrostatic atmospheric models called `COMARCS` . Then, using Equation 2 from Cruzalèbes et al. (2013) we estimate the Rosseland radius $R_\star = 5.3 \pm 0.6$ mas associated to the best fitting model. This last result is statistically consistent within $1.5\,\sigma$ with the radius estimated by Cruzalèbes et al. (2013) and Wittkowski et al. (2017).

The best-fitting `COMARCS` model is set as the central source for `DUSTY`. Then, we simultaneously fit photometric data and MATISSE visibilities. The resulting parameters of the fit, as well as their respective error bars, are given in Tab 1 and are consistent with the literature.

4. RHAPSODY and MIRA reconstruction

Two independent methods are used to locate the dusty and molecular regions: the `MIRA` 3D image reconstruction algorithm (Thiebaut & Giovannelli 2010) and the second one is a 1D new approach based on an intensity radial profile reconstruction method using the Hankel transform. The Hankel method has the advantage of requiring less parameters than image reconstruction, leading to less problems of non-uniqueness of the solution, a better convergence, and a better dynamic range, given that the source presents no or small asymmetries. In both case we reconstruct independent images, one per each spectral channel and we revealed some structures.

In the continuum around $3.50\,\mu$m and $10.00\,\mu$m, both reconstruction techniques (see Fig. 2 and Fig. 3) show a structure between 0–5 mas which can be interpreted as the star's photosphere and spectrally dominated by HCN molecules. Out of the continuum, in the molecular band features around $3.05\,\mu$m (C_2H_2+HCN) and $3.9\,\mu$m (C_2H_2), the structure apparent angular size increases up to 10 mas. This spectral region is characterized by strong asymmetries with non-zero closure phase observations near $3.1\ \mu$m as seen in Fig. 4.

Figure 3 shows that such asymmetries are signature of clumpy environment. Then, `RHAPSODY` underlines a structure between 12–18 mas visible only in $L-$ band and that
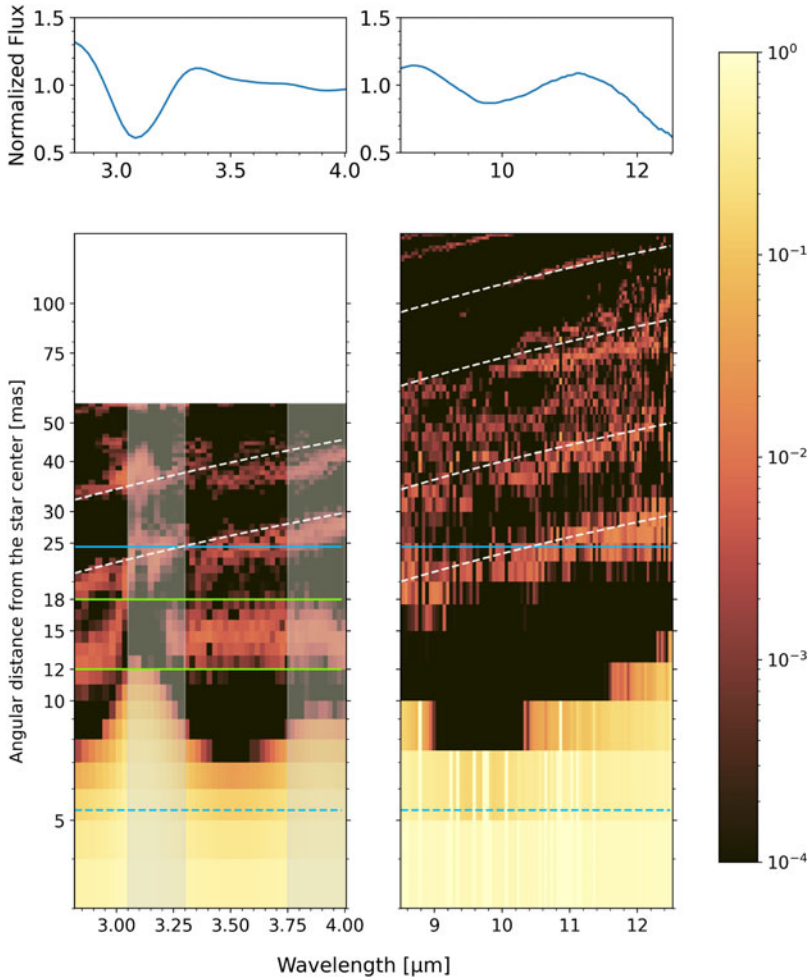
Figure 2. Upper panels correspond to the observed MATISSE spectrum normalized by the median and then divided by a black body spectra at T=2700 K to underline the observed emission and absorption features. Lower panels are the spectro-radial maps in *L*- and *N*-band obtained by plotting the best intensity Hankel profile normalized at one for each observed wavelength. The faint red structures highlighted with the inclined dashed-white lines are reconstruction artifacts. The dashed and solid blue horizontal lines show the position of the Rosseland radius and the `DUSTY` inner radius respectively. The solid green horizontal lines delimit the extension of a hot distinct molecular layer. The grey vertical bands cover the spectral ranges where the centro-symmetric Hankel profile is not able to properly reproduce the asymmetric shape of R Scl revealed by non-zero closure phases.

corresponding to the flux integration of all the clumpy structures visible on the `MIRA` image reconstruction. We speculate that such layer is composed by a mixture of molecules and first seeds of carbon dust grains. Finally, above 20 mas, `MIRA` shows asymmetric and clumpy structures as well as fuzzy emissions. Such structures could be filled by amorphous carbon (amC) or silicone carbide (SiC). However, we did not detected in the MATISSE visibilities structures related to SiC. Indeed, it is not clear at this point if the feature near $11.3\,\mu$m is induced by the superposition of continuum emission and molecular absorption or if it is truly an SiC dust feature.
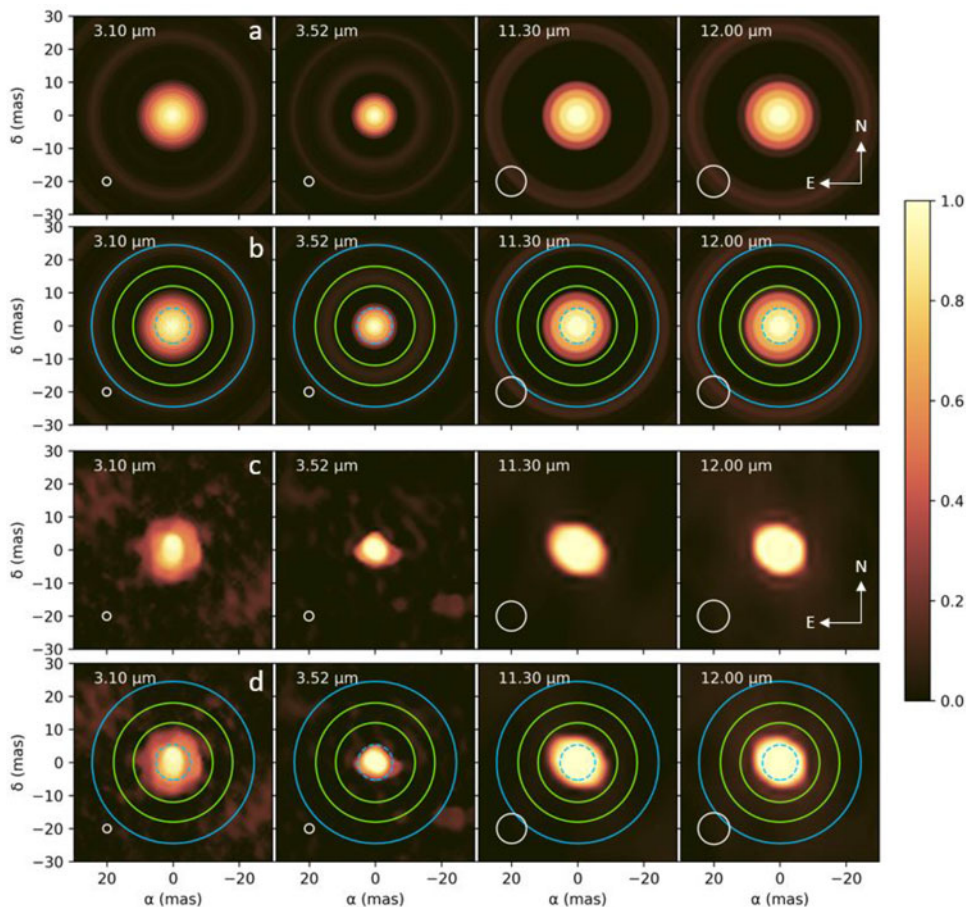
Figure 3. Reconstructed Hankel distribution from radial profiles (row a), the same with the identified features highlighted (row b), images reconstructed with MIRA (row c), and the same with features highlighted (row d). Each panel shows the reconstructed image at the wavelength shown at its left top corner, covering the L-band (3–$4\,\mu$m) and the N-band (8–$13\,\mu$m). In these panels, the blue dashed circle in the center shows the calculated Rosseland radius of the stellar photosphere, the green circles represent the inner and outer boundary of the distinct molecular shell (seen here only at $3.52\,\mu$m and only clearly identifiable in the Hankel reconstruction), the blue circle represents the inner boundary of the dust envelope predicted by DUSTY, while the white circle at each bottom left corner shows the theoretical angular resolution of the interferometer.

5. Results and Conclusion

The MATISSE spectra clearly show signatures possibly associated to acetylene (C_2H_2) and hydrogen cyanide (HCN) molecules at $3.1\,\mu$m as well as the solid state SiC at $11.3\,\mu$m (Yang et al. 2004). COMARCS and DUSTY allow us to estimate respectively the central source and the dust envelope properties. However this 1D composite modeling approach has strong limitations due to the strong assumptions and the complex nature of the source. Such limitations are seen for example in the quality of the L-band visibility fitting. MIRA and RHAPSODY provide good fit with MATISSE visibilities even in bandwidth where we expect strong molecular signatures. Both use different techniques: MIRA is a 3D image reconstruction code while RHAPSODY is a 1D intensity profile reconstruction code and provide consistent and complementary results between each others.

Similarities between PIONIER images and our results are found: in the continuum around
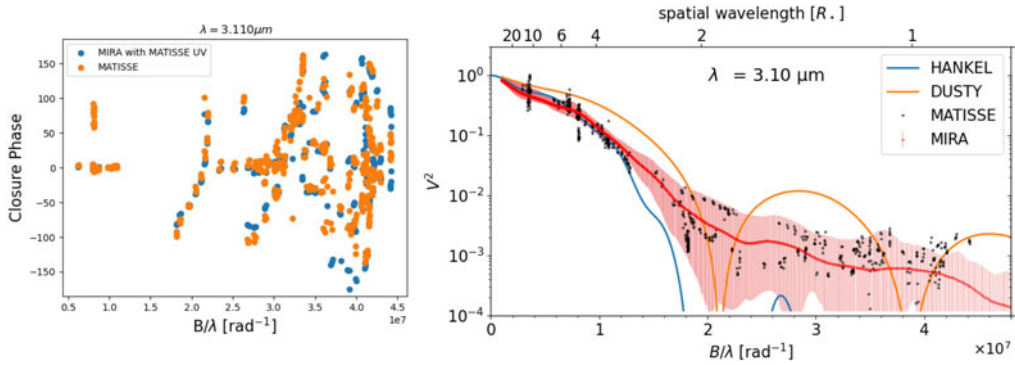
Figure 4. Left Panel: Comparison between the closure phase from the MIRA image reconstruction using the MATISSE (u,v)-plane coverage (blue dots) and the closure phase from MATISSE (orange dots). Right Panel: Plot of the MATISSE squared calibrated visibilities (grey dots) at $3.10\,\mu m$ around the C_2H_2+HCN absorption feature. We over-plotted the data with several models: Hankel profile (blue), DUSTY model (orange), and MIRA mean 1D radial profile (red) and its dispersion (solid red interval).

$3.5\,\mu m$ and $10.0\,\mu m$ we observe stellar disk of the same size. However, the MATISSE images are also characterize by strong asymmetries (i.e., clumpy structures) for example at $3.1\,\mu m$ where C_2H_2 and HCN are located. We also observe a distinct layer between 12–18 mas formed by molecules and dust which could be the result of an episodic mass-loss event. Concerning the dust, we don't find any clear spectral and spatial signature of SiC, then according also to the small amount of SiC involved in our SED fitting, we question the presence of SiC in the stellar radii probed by our observations. A comparison of our results with extended atmosphere models taking into account the simultaneous presence of gas and dust (Paladini et al. 2009) is subject of future work.

References

Aringer, B., Girardi, L., Nowotny, W., Marigo, P., & Bressan, A. 2016, MNRAS, 457, 3611

Brunner, M., Maercker, M., Mecina, M., Khouri, T., & Kerschbaum, F. 2018, A&A, 614, A17

Cruzalèbes, P., Jorissen, A., Rabbia, Y., et al. 2013, Monthly Notices of the Royal Astronomical Society, 434, 437

De Beck, E., Decin, L., de Koter, A., et al. 2010, A&A, 523, A18

Hron, J., Loidl, R., Hoefner, S., et al. 1998, A&A, 335, L69

Ivezić, Z. & Elitzur, M. 1996, MNRAS, 279, 1011

Lopez, B., Lagarde, S., Petrov, R. G., et al. 2022, A&A, accepted

Maercker, M., Brunner, M., Mecina, M., & De Beck, E. 2018, A&A, 611, A102

Maercker, M., Mohamed, S., Vlemmings, W. H. T., et al. 2012, Nature, 490, 232

Millour, F., Berio, P., Heininger, M., et al. 2016, in Society of Photo-Optical Instrumentation Engineers (SPIE) Conference Series, Vol. 9907, Optical and Infrared Interferometry and Imaging V, ed. F. Malbet, M. J. Creech-Eakman, & P. G. Tuthill, 990723

Paladini, C., Aringer, B., Hron, J., et al. 2009, A&A, 501, 1073

Sacuto, S., Aringer, B., Hron, J., et al. 2011, A&A, 525, A42

Samus, N. N., Kazarovets, E. V., Durlevich, O. V., Kireeva, N. N., & Pastukhova, E. N. 2009, VizieR Online Data Catalog, B/gcvs

Thiebaut, E. & Giovannelli, J. F. 2010, IEEE Signal Processing Magazine, 27, 97

Wittkowski, M., Hofmann, K. H., Höfner, S., et al. 2017, A&A, 601, A3

Yang, X., Chen, P., & He, J. 2004, A&A, 414, 1049

Yudin, R. V. & Evans, A. 2002, A&A, 391, 625